Division-linked generation of death-intermediates regulates the numerical stability of memory CD8 T cells

Jeffrey C. Nolz[a], Deepa Rai[b], Vladimir P. Badovinac[b,c,1], and John T. Harty[a,b,c,1,2]

Departments of [a]Microbiology and [b]Pathology and [c]Interdisciplinary Graduate Program in Immunology, University of Iowa, Iowa City, IA 52242

Edited by Philippa Marrack, Howard Hughes Medical Institute, National Jewish Health, Denver, CO, and approved March 8, 2012 (received for review November 16, 2011)

Infection or successful vaccination results in the formation of long-lived memory CD8 T-cell populations. Despite their numerical stability, memory CD8 T-cell populations are thought to completely turn over through proliferation within a 2- to 3-mo period. Therefore, steady-state memory cell proliferation must be balanced by a precisely regulated and equivalent death rate. However, the mechanisms regulating this balancing process remain completely undefined. Herein, we provide evidence for "death-intermediate memory cells" (T_{DIM}) within memory CD8 T-cell populations generated by infection. Importantly, CD62L^{Lo}/CD27^{Lo} T_{DIM}s are functionally characterized by an inability to produce cytokines, the failure to internalize T-cell receptor following antigenic stimulation, and signatures of apoptotic death. Furthermore, we demonstrate that, mechanistically, T_{DIM} are directly generated from dividing "central memory" T-cell populations undergoing memory turnover in vivo. Collectively, these results demonstrate that as central memory CD8 T cells proliferate, they continuously generate a population of CD8 T cells that are nonfunctional and apoptotic; thus, our data support a model wherein division-linked generation of T_{DIM} contributes to numerically stable CD8 T-cell memory.

Following infection or successful vaccination, naive CD8 T cells undergo a programmed series of biological events that ultimately result in the formation of long-lived memory populations (1–4). Independent of further antigenic stimulation (5, 6), memory CD8 T cells undergo modest rates of cellular proliferation driven by cytokines, such as IL-7 and IL-15 (7–12), and this "memory turnover" is critically important for maintaining stable memory CD8 T-cell numbers (1, 11). Despite their numerical stability, memory CD8 T-cell populations are thought to completely turn over through proliferation within a 2- to 3-mo period (13, 14). Thus, memory cell proliferation must be balanced by a precisely regulated and equivalent death rate. Although the relevance of stable memory maintenance for vaccination and immunity to infection is clear, the mechanisms and cellular intermediates in this balancing process remain completely undefined.

Multiple studies of memory CD8 T cells reveal that some cells within the population proliferate one or more times over an interval of several weeks (4, 13, 14). From a reductionist perspective, it is apparent that two basic models might account for the balancing act between proliferation and death that must occur to maintain stable CD8 T-cell numbers. In the first model (Fig. 1*A*, *Left*), one daughter cell generated by cytokine-driven division of a memory CD8 T cell lives, whereas the other daughter cell is destined to die. In the second model (Fig. 1*A*, *Right*), both daughter cells generated by division of a memory CD8 T cell live and one nondividing memory cell is destined to die. Thus, to begin to discriminate between these models, we sought to identify the CD8 T cells that are destined to die within a memory CD8 T-cell population.

Results

Nonfunctional Apoptotic Cells Are Found Within Memory CD8 T-Cell Populations. Memory CD8 T cells can rapidly produce a variety of cytokines, such as IFN-γ and TNF-α, following T-cell receptor (TCR) stimulation. In fact, production of IFN-γ following stimulation with peptide is often used to identify antigen-specific CD8 T cells following infection or vaccination (15). However, when splenic memory P14 TCR-transgenic (tg) CD8 T cells (Thy1.1$^+$, Vα2$^+$Vβ8.1$^+$) that were generated following lymphocytic choriomeningitis virus (LCMV) infection were stimulated with saturating amounts of $GP_{33–41}$ peptide (Fig. S1), a substantial proportion of these cells (~20–25%) failed to produce IFN-γ (Fig. 1*B*). This was not attributable to incomplete recruitment of the naive P14 CD8 T cells into the immune response or contamination with Thy1.1$^+$ cells expressing incorrect TCR, because low numbers of P14 cells were initially transferred, high numbers were recovered at memory time points, and all the Thy1.1$^+$ cells expressed the appropriate TCR (Vα2/Vβ8.1) (Fig. S1). We also found a similar percentage of memory CD8 T cells that failed to produce IFN-γ within two other TCR-tg T-cell populations (OT-I and CS_{280}-tg in C57BL/6 and BALB/c mice, respectively) following infection with *Listeria monocytogenes* expressing either the ovalbumin epitope, $OVA_{257–265}$, or the *Plasmodium yoelii* circumsporozoite protein epitope, $CS_{280–288}$, respectively (Fig. 1*B*). Costaining revealed that these IFN-γ$^-$ populations also failed to produce TNF-α and IL-2 (Fig. S2). Thus, the failure of a substantial proportion of cells to produce IFN-γ following peptide stimulation is a general feature of memory TCR-tg CD8 T-cell populations.

We next determined whether memory CD8 T cells that failed to produce IFN-γ exhibited a unique phenotype. Indeed, surface marker analysis revealed that >90% of IFN-γ–nonproducing memory P14 cells expressed low levels of both CD62L and CD27 (Fig. 1 *C* and *D*). Of note, the CD62L^{Lo}/CD27^{Lo} phenotype does not conclusively identify only cytokine nonproducing memory CD8 T cells, especially at early time points (i.e., day 40) following infection, but identifies the majority of these cells by day 150 postinfection with LCMV (Fig. S3). In addition to the failure to produce IFN-γ and the CD62L^{Lo}/CD27^{Lo} phenotype, this cell population was unable to undergo degranulation or internalize TCR following peptide stimulation (Fig. 1 *E* and *F*). Furthermore, this CD62L^{Lo}/CD27^{Lo} memory CD8 T-cell population did not undergo robust secondary expansion in vivo following LCMV infection, compared with CD62L^{Hi}/CD27^{Hi} "central memory" T cells (T_{CM}) [the dominant memory cell subset found at late time points (16)] (Fig. 1*G*). Therefore, these data demonstrate that the majority of CD62L^{Lo}/CD27^{Lo} memory CD8 T cells are nonfunctional at late time points following infection.

Failure of this cytokine "nonproducing" memory CD8 T-cell population to internalize TCR following antigenic stimulation suggested the possibility that insufficient proximal TCR signaling resulted in the inability to produce IFN-γ. However, although stimulation with phorbol 12-myristate 13-acetone (PMA)/

Author contributions: J.C.N., V.P.B., and J.T.H. designed research; J.C.N., D.R., and V.P.B. performed research; V.P.B. contributed new reagents/analytic tools; J.C.N., V.P.B., and J.T.H. analyzed data; and J.C.N., V.P.B., and J.T.H. wrote the paper.

The authors declare no conflict of interest.

This article is a PNAS Direct Submission.

[1]V.P.B. and J.T.H. contributed equally to this work.

[2]To whom correspondence should be addressed. E-mail: john-harty@uiowa.edu.

This article contains supporting information online at www.pnas.org/lookup/suppl/doi:10.1073/pnas.1118868109/-/DCSupplemental.

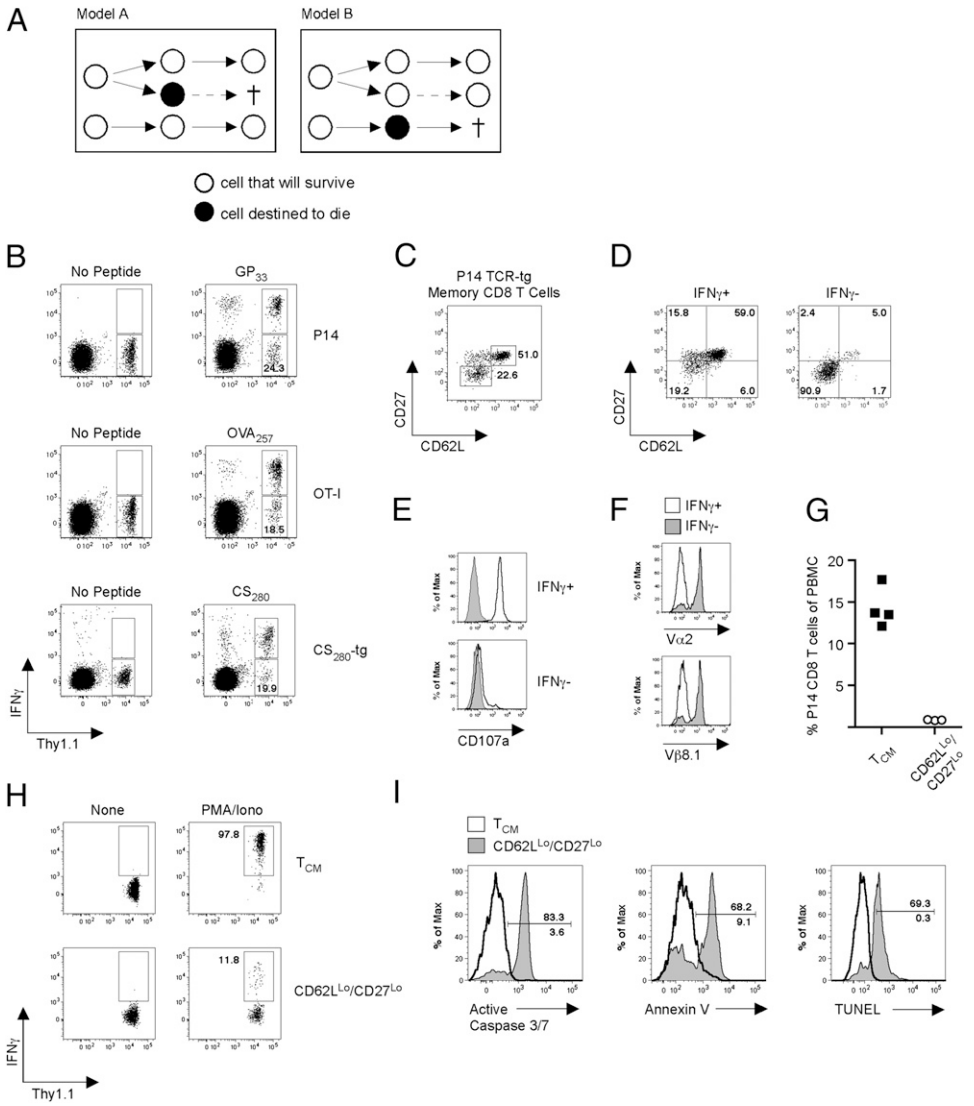

Fig. 1. Identification of functionally impaired CD8 T cells within a population of TCR-tg memory CD8 T cells. (*A*) Proposed models for the numerical stability of memory CD8 T-cell populations during steady-state proliferation. (*B*) B6 or BALB/c mice (Thy1.2) that had received a physiological number (500–5,000) of the indicated TCR-tg CD8 T cells (Thy1.1) were analyzed for TCR-tg T-cell production of IFN-γ following peptide stimulation. Analysis was performed at least 80 d following the indicated infection. [B6, P14 CD8 T cells, LCMV–Armstrong infection (*Top*); B6, OT-I CD8 T cells, *Listeria monocytogenes* (LM)-OVA infection (*Middle*); BALB/c, CS_{280}-tg, LM-CS infection (*Bottom*)]. (*C*) Expression of CD62L and CD27 on total Thy1.1 memory P14 CD8 T cells 120 d after LCMV–Armstrong infection. (*D*) Ex vivo stimulation with $GP_{33–41}$ peptide was performed as in *B*, with the exception that N-(R)-(2-(Hydroxyaminocarbonyl)methyl)-4-methylpentanoyl-L-*t*-butyl-glycine-L-alanine 2-aminoethyl amide was added to inhibit CD62L cleavage. Expression of CD62L and CD27 was then determined on IFN-γ^+ and IFN-γ^- memory P14 CD8 T cells. (*E*) Same as in *D*, with the exception that cells were analyzed for their ability to degranulate through surface expression of CD107a. (*F*) Same as in *D*, with the exception that surface expression of Vα2 or Vβ8.1 TCR levels on P14 CD8 T cells was determined following ex vivo stimulation with $GP_{33–41}$ peptide. (*G*) $CD62L^{Hi}/CD27^{Hi}$ T_{CM} and $CD62L^{Lo}/CD27^{Lo}$ memory P14 CD8 T cells were purified by FACS from spleens of LCMV-infected animals and transferred into naive B6 recipients. Secondary expansion of the transferred cell populations was analyzed in the blood on day 7 postinfection with LCMV. PBMC, peripheral blood mononuclear cell. (*H*) Production of IFN-γ was analyzed in T_{CM} and $CD62L^{Lo}/CD27^{Lo}$ memory P14 CD8 T cells following stimulation with PMA and ionomycin (Iono). (*I*) Analysis of apoptosis of T_{CM} and $CD62L^{Lo}/CD27^{Lo}$ memory P14 CD8 T cells by activation of caspase-3/7, Annexin V staining, and TUNEL. All data are representative of multiple mice analyzed in independent experiments performed three or more times.

ionomycin resulted in IFN-γ production by >97% of T_{CM} CD8 T cells, only a small fraction of $CD62L^{Lo}/CD27^{Lo}$ memory cells made detectable cytokine, suggesting that the inability to produce cytokine was not attributable to impaired proximal TCR signaling (Fig. 1*H*). Because this unique cell population failed to exhibit major functional characteristics of memory CD8 T cells (cytokine production, degranulation, and secondary responses), we next determined whether the $CD62L^{Lo}/CD27^{Lo}$ memory cells exhibited hallmark features of apoptosis. Indeed, compared with T_{CM} in the same samples, $CD62L^{Lo}/CD27^{Lo}$ memory CD8 T cells displayed substantially more activated caspase-3 and caspase-7, surface expression of phosphatidylserine, and DNA fragmentation (Fig. 1*I*). Collectively, these data suggest that the $CD62L^{Lo}/CD27^{Lo}$ memory CD8 T cells that cannot produce IFN-γ are highly susceptible to apoptosis.

As shown in Fig. 1*F*, this unique cell population fails to internalize TCR; thus, it can still be detected using H2-D^b-GP_{33} tetramer staining following peptide stimulation (Fig. S4*A*). Indeed, following stimulation with $GP_{33–41}$ peptide, memory P14 CD8 T cells that remained tetramer-positive were $CD62L^{Lo}/CD27^{Lo}$, did not make IFN-γ, and did not internalize TCR (Fig. S4 *B–D*). Thus, we used this approach to determine whether a population of nonfunctional apoptotic memory CD8 T cells was present in an endogenous memory population. We infected B6 mice with LCMV; at a memory time point, we stimulated their splenocytes with saturating amounts of $GP_{33–41}$ peptide. This resulted in robust IFN-γ production and a substantial decrease in the percentage of CD8 T cells that could be detected with H2-D^b-GP_{33} tetramer (Fig. 2*A*). Strikingly, cells that failed to internalize TCR (remained tetramer-positive) following antigen stimulation exhibited a uniform $CD62L^{Lo}/CD27^{Lo}$ phenotype identical to that observed in the cytokine nonproducing TCR-tg memory CD8 T-cell populations (Fig. 2 *A* and *B*). In contrast, the T_{CM} population could no longer be detected, suggesting that this cell population efficiently internalized TCR following peptide stimulation. Similar results were found for memory populations specific for the LCMV NP_{396} and GP_{276} epitopes (Fig. 2*B*). In addition, a large percentage of $CD62L^{Lo}/CD27^{Lo}$ endogenous memory CD8 T cells displayed activation of caspase-3 and caspase-7 (Fig. 2*C*). Thus, these functionally impaired apoptotic $CD62L^{Lo}/CD27^{Lo}$ CD8 T cells are found in both TCR-tg and endogenous memory CD8 T-cell populations.

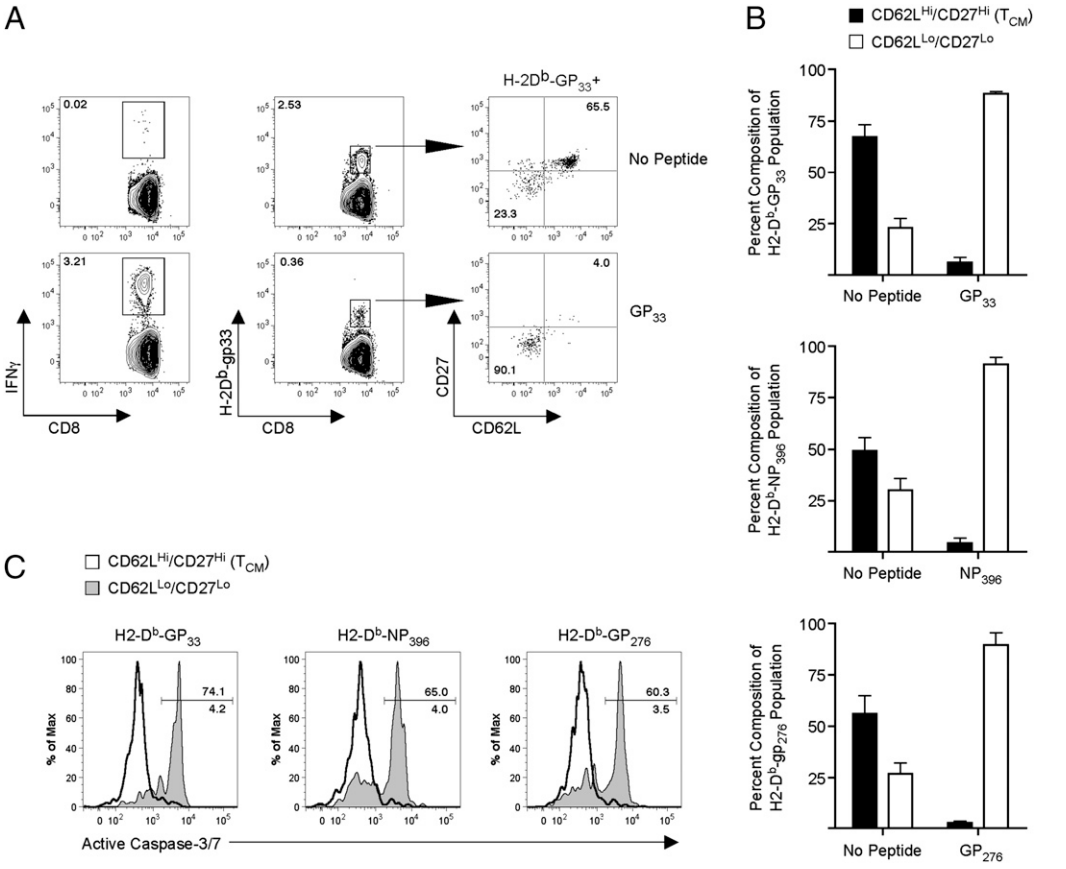

Fig. 2. Functionally impaired CD62L^{Lo}/CD27^{Lo} cells can be detected in the endogenous repertoire of memory CD8 T-cell populations. (*A*) IFN-γ production and the ability to bind H2-D^b-GP$_{33}$ tetramer were determined following stimulation with GP$_{33–41}$ peptide in day 150 memory CD8 T cells from LCMV-infected B6 mice. Expression of CD62L and CD27 was then analyzed on H2-D^b-GP$_{33}$ tetramer-positive CD8 T cells. (*B*) Quantification of the percentage of H2-D^b-GP$_{33}$, H2-D^b-NP$_{396}$, and H2-D^b-GP$_{276}$ tetramer-positive CD8 T cells that expressed CD62L and CD27 following no stimulation or stimulation with the corresponding peptide. (*C*) Analysis of activation of caspase-3/7 on LCMV-specific tetramer-positive cells. Data are representative of two independent experiments.

Memory CD8 T Cells That Cannot Produce IFN-γ Are Phenotypically and Functionally Distinct from Effector Memory Cells. "Effector" and "effector memory" CD8 T cells (T$_{EM}$) do not express CD62L and are often CD27^{Lo} (16–20). In fact, as shown in Fig. S3, a substantial proportion of CD62L^{Lo}/CD27^{Lo} memory CD8 T cells produce IFN-γ, especially at early memory time points following infection. Therefore, we next determined whether there were additional phenotypic differences that could discriminate between the CD62L^{Lo}/CD27^{Lo} populations based on their ability to produce cytokines following stimulation with peptide (Fig. 3*A*). Low expression of CD127 and high expression of KLRG1 are often used to identify effector CD8 T-cell populations following infection (21–23). Indeed, CD62L^{Lo}/CD27^{Lo} memory CD8 T cells that produced IFN-γ following stimulation with peptide expressed high levels of KLRG1 and low levels of CD127 (Fig. 3*B*). In contrast, CD62L^{Lo}/CD27^{Lo} memory CD8 T cells that did not produce IFN-γ exhibited the opposite phenotype and expressed low levels of KLRG1 and high levels of CD127, similar to T$_{CM}$ (Fig. 3*B*). Thus, these data suggest that memory CD8 T cells that cannot produce IFN-γ are CD62L^{Lo}/CD27^{Lo}/CD127^{Hi}/KLRG1^{Lo}, demonstrating that they are phenotypically distinct from effector and T$_{EM}$ CD8 T cells.

As a result of changes in homing receptors, T$_{CM}$ and T$_{EM}$ exhibit different localization patterns within host tissues. To address the localization of the cytokine nonproducing memory population, we analyzed the ability for the CD62L^{Lo}/CD27^{Lo}

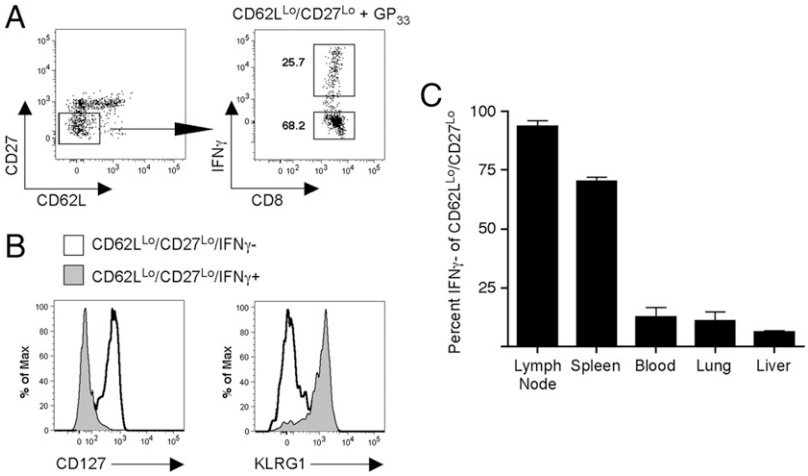

Fig. 3. Functionally impaired CD62L^{Lo}/CD27^{Lo} memory CD8 T cells are found in lymphoid organs and are phenotypically distinct from "effector memory." (*A*) 5×10^3 naive P14 CD8 T cells were transferred into B6 mice and subsequently infected with LCMV–Armstrong. On day 50 postinfection, CD62L^{Lo}/CD27^{Lo} memory P14 CD8 T cells from the spleen were analyzed for the ability to produce IFN-γ following GP$_{33–41}$ stimulation. (*B*) Using the gating strategy shown in *A*, expression of CD127 (*Left*) and KLRG1 (*Right*) was analyzed on IFN-γ$^+$ and IFN-γ$^-$ cells within the CD62L^{Lo}/CD27^{Lo} population. (*C*) Same as in *A*, with the exception that memory P14 CD8 T cells were analyzed from the indicated tissue. The percentage of IFN-γ$^-$ cells following GP$_{33–41}$ stimulation within the CD62L^{Lo}/CD27^{Lo} population was quantified. Representative dot plots are shown in Fig. S5. Data are representative of two independent experiments.

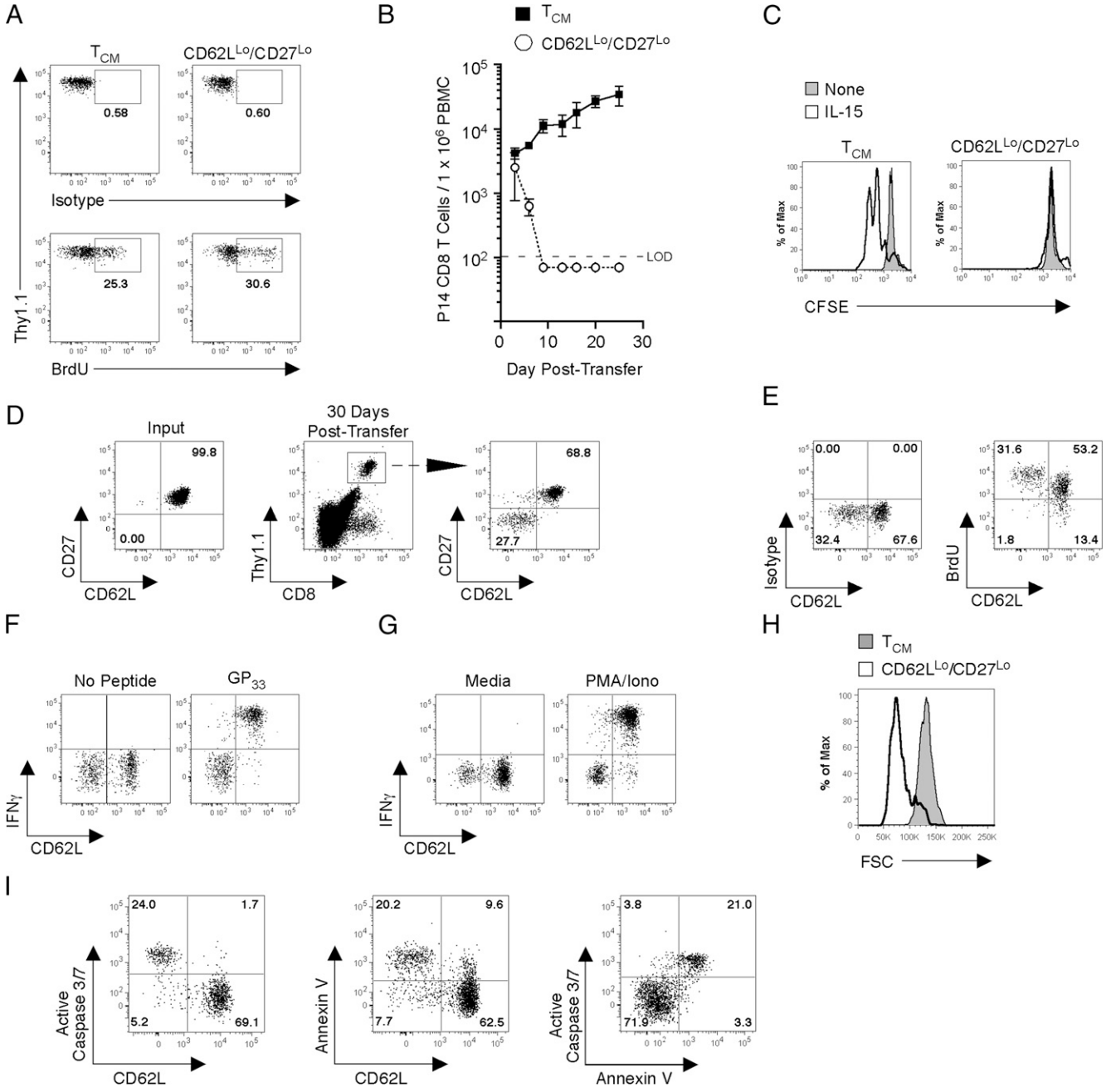

Fig. 4. Functionally impaired CD62L^{Lo}/CD27^{Lo} cells are generated during homeostatic proliferation of CD62L^{Hi}/CD27^{Hi} T_{CM} CD8 T cells. (*A*) 5×10^3 naive P14 CD8 T cells were transferred into B6 mice and subsequently infected with LCMV–Armstrong. At 135 d postinfection, mice were placed on drinking water containing BrdU for 15 d. Cellular proliferation, determined by incorporation of BrdU, was then analyzed on CD62L^{Hi}/CD27^{Hi} (T_{CM}) and CD62L^{Lo}/CD27^{Lo} memory P14 CD8 T cells. (*B*) 1.5×10^5 T_{CM} or CD62L^{Lo}/CD27^{Lo} memory P14 CD8 T cells were FACS-sorted from the spleen and transferred into Rag1$^{-/-}$ B6 mice. Total cell numbers in the blood were then monitored longitudinally. Error bars indicate SD of three mice per group. LOD, limit of detection. (*C*) Cells were sorted as in *B* and labeled with CFSE. Proliferation was then analyzed on the sorted populations following 3 d of stimulation in vitro with 200 ng/mL IL-15. (*D*) 2.5×10^5 T_{CM} P14 CD8 T cells were sorted by FACS and transferred into Rag1$^{-/-}$ B6 mice. Thirty days after transfer, the adoptively transferred population was analyzed for expression of CD62L and CD27. (*E*) Same as in *D*, with the exception that incorporation of BrdU was determined following pulse on days 10–25 after transfer. (*F* and *G*) Same as in *D*, with the exception that IFN-γ production was determined following stimulation with GP$_{33-41}$ peptide (*F*) or PMA and ionomycin (Iono) (*G*). (*H*) Same as in *D*, with the exception that cell size was determined based on forward scatter (FSC) on the two cell populations. (*I*) Same as in *D*, with the exception that activation of caspase-3 and caspase-7 and annexin V staining were analyzed on the adoptively transferred population. All data are representative of three independent experiments.

memory P14 CD8 T cells from blood, lymphoid organs, and peripheral tissues to produce IFN-γ. On day 60 postinfection with LCMV, ~75% of the CD62L^{Lo}/CD27^{Lo} memory CD8 T-cell population in the spleen did not make IFN-γ following stimulation with GP$_{33}$ peptide (Fig. 3*C* and Fig. S5). Furthermore, nearly all the CD62L^{Lo}/CD27^{Lo} memory CD8 T cells in the lymph node failed to produce IFN-γ. In contrast, in both the blood and peripheral tissues (liver and lung), >90% of the memory CD8 T cells that were CD62L^{Lo}/CD27^{Lo} produced IFN-γ following stimulation with peptide. Overall, these data demonstrate that

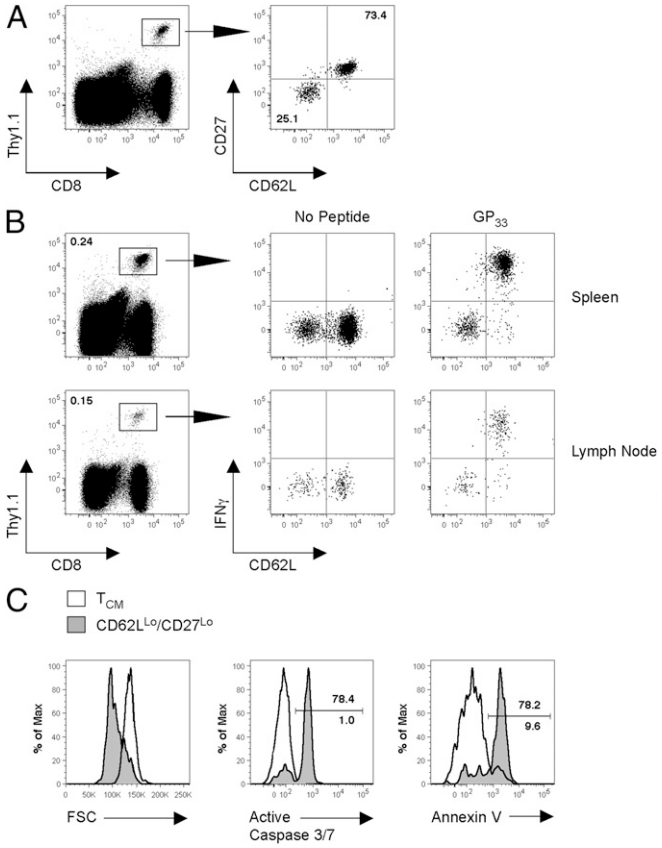

Fig. 5. Functionally impaired CD62L^{Lo}/CD27^{Lo} cells are generated following transfer of T_{CM} CD8 T cells into WT mice. (*A*) CD62L^{Hi}/CD27^{Hi} T_{CM} P14 CD8 T cells were sorted (>99% purity) as shown in Fig. 4*D* and transferred into WT B6 mice. Thirty-five days after transfer, the adoptively transferred population was analyzed for expression of CD62L and CD27. (*B*) Same as in *A*, with the exception that production of IFN-γ was analyzed on the adoptively transferred population following stimulation with GP_{33-41} peptide from cells isolated from either the spleen or inguinal lymph node. (*C*) Same as in *A*, with the exception that cell size by forward scatter (FSC), activation of caspase-3 and caspase-7, and annexin V staining were analyzed on the adoptively transferred population. Data are representative of two independent experiments.

this unique CD62L^{Lo}/CD27^{Lo} memory CD8 T-cell population is found predominantly within lymphoid tissues, such as the spleen and lymph nodes.

CD62L^{Lo}/CD27^{Lo} Memory CD8 T Cells Do Not Undergo Homeostatic Proliferation. Sustained but relatively slow proliferation is thought to be critical in maintaining the long-term numerical stability in memory CD8 T-cell populations observed in both humans and laboratory mice (24–26). Because cytokine nonproducing memory CD8 T cells exhibited the molecular signatures of apoptosis, we next determined whether these functionally impaired memory CD8 T cells were undergoing proliferation in vivo at late time points (>150 d postinfection with LCMV). Surprisingly, a similar fraction of CD62L^{Lo}/CD27^{Lo} memory cells incorporated BrdU over a 2-wk period compared with the highly proliferative T_{CM} subpopulation. Thus, the CD62L^{Lo}/CD27^{Lo} memory cells had gone through at least one cell division during that time interval (Fig. 4*A*). However, when T_{CM} and CD62L^{Lo}/CD27^{Lo} memory CD8 T cells were purified and transferred into separate groups of lymphopenic Rag1$^{-/-}$ recipients (to drive rapid homeostatic proliferation), only T_{CM}, and not the CD62L^{Lo}/CD27^{Lo} cells, expanded in the new hosts (Fig. 4*B*). In fact, the few CD62L^{Lo}/CD27^{Lo} memory CD8 T cells found at day 3 after transfer could no longer be detected in the Rag1$^{-/-}$ recipients on day 9 after transfer. In addition, CD62L^{Lo}/CD27^{Lo} memory cells failed to undergo proliferation in vitro in response to IL-15 stimulation, whereas T_{CM} readily underwent cell division (Fig. 4*C*). Therefore, these data suggest that consistent with their nonfunctional and apoptotic phenotype, this unique population of CD62L^{Lo}/CD27^{Lo} memory CD8 T cells does not undergo proliferation and does not survive in vivo. Instead, these data suggest that the CD62L^{Lo}/CD27^{Lo} memory CD8 T-cell population may be generated as a byproduct of T_{CM} turnover.

Proliferating T_{CM} CD8 T Cells Continuously Generate Nonfunctional Apoptotic Cells. Because the overall number of memory CD8 T cells remains constant over long periods of time, the observed continual proliferation of memory CD8 T cells must be accompanied by a nearly equal death rate. Indeed, highly purified (>99%) T_{CM} transferred into Rag1$^{-/-}$ mice undergo substantial proliferation (Fig. 4*B*). Strikingly, when the adoptively transferred T_{CM} population was analyzed 30 d after transfer for expression of CD62L and CD27, a substantial proportion of the transferred T_{CM} CD8 T cells (CD62L^{Hi}/CD27^{Hi}) now exhibited a CD62L^{Lo}/CD27^{Lo} phenotype and all these newly generated cells had proliferated following transfer (Fig. 4 *D* and *E*). In addition, the CD62L^{Lo}/CD27^{Lo} CD8 T cells that were generated following transfer failed to produce IFN-γ following stimulation with either peptide or PMA/ionomycin, whereas the cells that exhibited the T_{CM} phenotype uniformly produced this cytokine (Fig. 4 *F* and *G*). Finally, the CD62L^{Lo}/CD27^{Lo} memory cells that appeared following transfer exhibited hallmarks of apoptosis, including reduced size (as measured by forward scatter), activation of caspase-3 and caspase-7, and surface phosphatidylserine expression (Fig. 4 *H* and *I*). Thus, these data would argue that memory CD8 T cells that cannot produce cytokines and exhibit the hallmarks of apoptosis are directly generated from T_{CM} populations undergoing homeostatic proliferation.

Generation of impaired memory CD8 T cells from a fully functional T_{CM} population following transfer into Rag1$^{-/-}$ mice suggested that these cells were byproducts of cell division. However, because the lymphopenic Rag1$^{-/-}$ environment results in robust homeostatic proliferation that exceeds normal memory turnover in a WT host, we next tested whether functionally impaired CD62L^{Lo}/CD27^{Lo} memory CD8 T cells could be generated from T_{CM} following transfer into a WT environment. Indeed, at 35 d following transfer of T_{CM} into a WT host, a substantial percentage of the recovered cells now exhibited the CD62L^{Lo}/CD27^{Lo} phenotype (Fig. 5*A*). In addition, these newly generated cells that were found in both the spleen and lymph node were unable to produce IFN-γ in response to antigenic stimulation (Fig. 5*B*). Finally, the CD62L^{Lo}/CD27^{Lo} cells generated from T_{CM} in WT hosts also exhibited characteristics of apoptosis, including reduced size, activation of caspase-3 and caspase-7, and expression of surface phosphatidylserine (Fig. 5*C*). Therefore, these data demonstrate that nonfunctional apoptotic CD62L^{Lo}/CD27^{Lo} memory CD8 T cells are generated from T_{CM} during memory turnover in WT hosts.

Discussion

Persistence of stable numbers of memory CD8 T-cell populations has long been appreciated as a hallmark characteristic of cellular immunity. In addition, the ability to "self-renew" through steady-state proliferation has been recognized as being critical for maintaining a constant number of memory CD8 T cells for long periods of time. In fact, memory CD8 T-cell populations numerically decline at a slow rate when steady-state proliferation is diminished (7–12). On the contrary, because memory CD8 T-cell populations remain quantitatively stable, this proliferation must be balanced by a tightly regulated rate of cell death; otherwise, memory CD8 T-cell populations would gradually inflate over time. However, until now, models to explain how

memory CD8 T-cell numbers are maintained in the face of memory turnover have not been experimentally addressed.

Herein, we demonstrate that a nonfunctional apoptotic subset of cells is a general feature of memory CD8 T-cell populations that form following infection. Mechanistically, we provide direct evidence that as T_{CM} CD8 T cells turn over by proliferation, they generate this population of cells that lack functionality and exhibit signatures of apoptosis. Thus, we would argue that this newly identified memory CD8 T-cell subset constitutes a previously unidentified "death-intermediate memory" (T_{DIM}) population, generated during memory turnover, that will ultimately die, and thus contribute a critical regulatory event in maintaining the numerical stability in memory CD8 T-cell populations. Furthermore, we show that generation of the T_{DIM} population can be linked to cell division of T_{CM} during memory turnover. Therefore, our data support an important role for a division-linked model wherein memory turnover produces two different daughter cells: a "renewed" T_{CM} and a T_{DIM} (Fig. 1*A*, *Left*). Whether this division-linked mechanism is the sole pathway for regulating CD8 T-cell numbers during all phases of the memory immune response remains to be determined. However, identification of the T_{DIM} population provides a potential "missing link" that will permit future studies aimed to determine their precise cellular origins.

Additionally, our results open a unique avenue for future studies aimed at understanding the specific molecular and cellular mechanisms that regulate the process of T_{DIM} formation. One possibility is that the T_{DIM} population is simply unable to compete adequately for survival cytokines, which then causes it to become apoptotic. However, our data suggest this is not the case, because this population still forms during memory CD8 T-cell proliferation in the noncompetitive $Rag1^{-/-}$ environment. Therefore, T_{DIM} generation is likely the result of changes in either gene regulation or the activation of signaling pathways that occur during or following cell division. In fact, several recent studies have suggested that asymmetrical cell division is a general feature of CD8 T cells that occurs following stimulation of the TCR (27–29). However, whether asymmetrical cell division occurs in proliferating memory CD8 T cells in a TCR-independent fashion is currently unknown. Overall, a complete understanding of the intrinsic and/or extrinsic signals that regulate generation of T_{DIM} populations might ultimately lead to therapies that could increase the quantity of memory CD8 T-cell populations.

Materials and Methods

Mice and Pathogens. C57BL/6 and BALB/c mice were obtained form the National Cancer Institute and used for experiments at 6–10 wk of age. P14 (30), OT-I (31), and CS_{280}-tg (32) mice have previously been described and maintained by sibling × sibling mating. $Rag1^{-/-}$ mice (33) were obtained from the Jackson Laboratories. LCMV–Armstrong was propagated according to standard protocols and injected (2×10^5 plaque-forming units) i.p. as indicated. Attenuated *Listeria monocytogenes* expressing OVA or CS protein from *P. yoelii* have been previously described (34, 35). Attenuated *L. monocytogenes* were injected i.v. at a dose of 1×10^7 cfu. All animal experiments followed approved Institutional Animal Care and Use Committee protocols.

Additional methods can be found in *SI Materials and Methods*.

ACKNOWLEDGMENTS. We thank members of the J.T.H. and V.P.B. laboratories for helpful discussion and Stanley Perlman for critical review of the manuscript. We also thank the University of Iowa Flow Cytometry Facility for cell sorting. This work was supported by National Institutes of Health Grants AI42767, AI46653, AI50073, AI085515 (to J.T.H.), and AI83286 (to V.P.B.) and a Career Development Award from the Leukemia and Lymphoma Society (to J.C.N.).

1. Harty JT, Badovinac VP (2008) Shaping and reshaping CD8+ T-cell memory. *Nat Rev Immunol* 8:107–119.
2. Badovinac VP, Harty JT (2006) Programming, demarcating, and manipulating CD8+ T-cell memory. *Immunol Rev* 211:67–80.
3. Kaech SM, Wherry EJ (2007) Heterogeneity and cell-fate decisions in effector and memory CD8+ T cell differentiation during viral infection. *Immunity* 27:393–405.
4. Williams MA, Holmes BJ, Sun JC, Bevan MJ (2006) Developing and maintaining protective CD8+ memory T cells. *Immunol Rev* 211:146–153.
5. Murali-Krishna K, et al. (1999) Persistence of memory CD8 T cells in MHC class I-deficient mice. *Science* 286:1377–1381.
6. Leignadier J, Hardy MP, Cloutier M, Rooney J, Labrecque N (2008) Memory T-lymphocyte survival does not require T-cell receptor expression. *Proc Natl Acad Sci USA* 105:20440–20445.
7. Schluns KS, Kieper WC, Jameson SC, Lefrançois L (2000) Interleukin-7 mediates the homeostasis of naïve and memory CD8 T cells in vivo. *Nat Immunol* 1:426–432.
8. Schluns KS, Williams K, Ma A, Zheng XX, Lefrançois L (2002) Cutting edge: Requirement for IL-15 in the generation of primary and memory antigen-specific CD8 T cells. *J Immunol* 168:4827–4831.
9. Becker TC, et al. (2002) Interleukin 15 is required for proliferative renewal of virus-specific memory CD8 T cells. *J Exp Med* 195:1541–1548.
10. Surh CD, Sprent J (2008) Homeostasis of naive and memory T cells. *Immunity* 29: 848–862.
11. Schluns KS, Lefrançois L (2003) Cytokine control of memory T-cell development and survival. *Nat Rev Immunol* 3:269–279.
12. Goldrath AW, et al. (2002) Cytokine requirements for acute and Basal homeostatic proliferation of naive and memory CD8+ T cells. *J Exp Med* 195:1515–1522.
13. Choo DK, Murali-Krishna K, Anita R, Ahmed R (2010) Homeostatic turnover of virus-specific memory CD8 T cells occurs stochastically and is independent of CD4 T cell help. *J Immunol* 185:3436–3444.
14. Parretta E, et al. (2008) Kinetics of in vivo proliferation and death of memory and naive CD8 T cells: Parameter estimation based on 5-bromo-2′-deoxyuridine incorporation in spleen, lymph nodes, and bone marrow. *J Immunol* 180:7230–7239.
15. Murali-Krishna K, et al. (1998) Counting antigen-specific CD8 T cells: A reevaluation of bystander activation during viral infection. *Immunity* 8:177–187.
16. Wherry EJ, et al. (2003) Lineage relationship and protective immunity of memory CD8 T cell subsets. *Nat Immunol* 4:225–234.
17. Appay V, et al. (2002) Memory CD8+ T cells vary in differentiation phenotype in different persistent virus infections. *Nat Med* 8:379–385.
18. Bouneaud C, Garcia Z, Kourilsky P, Pannetier C (2005) Lineage relationships, homeostasis, and recall capacities of central- and effector-memory CD8 T cells in vivo. *J Exp Med* 201:579–590.
19. Marzo AL, et al. (2005) Initial T cell frequency dictates memory CD8+ T cell lineage commitment. *Nat Immunol* 6:793–799.
20. Masopust D, Ha SJ, Vezys V, Ahmed R (2006) Stimulation history dictates memory CD8 T cell phenotype: Implications for prime-boost vaccination. *J Immunol* 177:831–839.
21. Kaech SM, et al. (2003) Selective expression of the interleukin 7 receptor identifies effector CD8 T cells that give rise to long-lived memory cells. *Nat Immunol* 4: 1191–1198.
22. Huster KM, et al. (2004) Selective expression of IL-7 receptor on memory T cells identifies early CD40L-dependent generation of distinct CD8+ memory T cell subsets. *Proc Natl Acad Sci USA* 101:5610–5615.
23. Joshi NS, et al. (2007) Inflammation directs memory precursor and short-lived effector CD8(+) T cell fates via the graded expression of T-bet transcription factor. *Immunity* 27:281–295.
24. Sallusto F, Lanzavecchia A, Araki K, Ahmed R (2010) From vaccines to memory and back. *Immunity* 33:451–463.
25. Homann D, Teyton L, Oldstone MB (2001) Differential regulation of antiviral T-cell immunity results in stable CD8+ but declining CD4+ T-cell memory. *Nat Med* 7: 913–919.
26. Hammarlund E, et al. (2003) Duration of antiviral immunity after smallpox vaccination. *Nat Med* 9:1131–1137.
27. Chang JT, et al. (2007) Asymmetric T lymphocyte division in the initiation of adaptive immune responses. *Science* 315:1687–1691.
28. Oliaro J, et al. (2010) Asymmetric cell division of T cells upon antigen presentation uses multiple conserved mechanisms. *J Immunol* 185:367–375.
29. Chang JT, et al. (2011) Asymmetric proteasome segregation as a mechanism for unequal partitioning of the transcription factor T-bet during T lymphocyte division. *Immunity* 34:492–504.
30. Pircher H, Bürki K, Lang R, Hengartner H, Zinkernagel RM (1989) Tolerance induction in double specific T-cell receptor transgenic mice varies with antigen. *Nature* 342: 559–561.
31. Hogquist KA, et al. (1994) T cell receptor antagonist peptides induce positive selection. *Cell* 76:17–27.
32. Sano G, et al. (2001) Swift development of protective effector functions in naive CD8 (+) T cells against malaria liver stages. *J Exp Med* 194:173–180.
33. Mombaerts P, et al. (1992) RAG-1-deficient mice have no mature B and T lymphocytes. *Cell* 68:869–877.
34. Haring JS, Badovinac VP, Olson MR, Varga SM, Harty JT (2005) In vivo generation of pathogen-specific Th1 cells in the absence of the IFN-gamma receptor. *J Immunol* 175: 3117–3122.
35. Butler NS, Schmidt NW, Harty JT (2010) Differential effector pathways regulate memory CD8 T cell immunity against Plasmodium berghei versus P. yoelii sporozoites. *J Immunol* 184:2528–2538.

Supporting Information

Nolz et al. 10.1073/pnas.1118868109

SI Materials and Methods

BrdU Incorporation. Mice were injected i.p. with 2 mg of BrdU (Sigma–Aldrich) at the beginning of the time period studied and subsequently given drinking water containing 0.8 mg/mL BrdU. At the time points indicated, T-cell proliferation was assessed in spleen samples using the FITC BrdU Flow Kit (BD Pharmingen) according to the manufacturer's protocols. Cells were analyzed on a FACSCanto flow cytometer (BD Biosciences).

Cell Purification and Adoptive Transfer. To purify memory P14 CD8 T-cell populations for adoptive transfer, single-cell suspensions of total splenocytes from mice containing Thy1-disparate primary memory P14 CD8 T cells were stained with phycoerythrin (PE)–anti-Thy1.1 antibody (Clone OX-7; BD Pharmingen), allophycocyanin–anti-CD62L antibody (Clone MEL-14; BD Pharmingen), and FITC–anti-CD27 antibody (Clone LG.7F9; eBioscience) in PBS containing 5% (vol/vol) FCS. Memory cells were then purified with anti-PE magnetic bead sorting using standard Automacs protocols (Miltenyi Biotec). Following AutoMacs purification, subpopulations of memory P14 CD8 T cells were sorted using a Becton Dickinson ARIA II cell sorter (1).

In Vitro Proliferation. Sorted memory P14 CD8 T cells were stained with 1 μM carboxyfluorescein succinimidylester (CFSE) for 15 min and thoroughly washed with RPMI containing 10% (vol/vol) FCS. Then, 1×10^4 cells were incubated for 72 h with or without 200 ng/mL IL-15 (Peprotech). Proliferation was then assessed by CFSE dilution.

Ex Vivo Cytokine Production. Analysis of IFN-γ production by antigen-specific CD8 T cells was performed essentially as previously described (2). Briefly, 2×10^6 total splenocytes were incubated for 5 h with or without saturating amounts (>200 nM) of the indicated peptide or for 4 h with PMA (50 ng/mL) and ionomycin (500 ng/mL) in the presence of Brefeldin A. Intracellular cytokine staining was then performed using the BD Cytofix/Cytoperm kit (Becton Dickinson) according to the manufacturer's protocol. In cases in which expression of CD62L was analyzed in combination with intracellular cytokine stain, cells were treated with 100 μM *N*-(R)-(2-(Hydroxyaminocarbonyl) methyl)-4-methylpentanoyl-L-t-butyl-glycine-L-alanine 2-aminoethyl amide (Peptides International), before addition of peptide and Brefeldin A, to inhibit cleavage of CD62L (3).

Analysis of Apoptosis. Detection of active caspase-3 and caspase-7 was determined using the Vybrant FAM Caspase-3 and Caspase-7 Assay Kit (Invitrogen) according to the manufacturer's protocol. Briefly, $\sim 2 \times 10^6$ total splenocytes were incubated for 1 h in 300 μL of RPMI containing 10% (vol/vol) FCS and 1× FLICA reagent at 37 °C. Cells were then thoroughly washed before being stained with additional antibodies against cell surface antigens. Detection of Annexin V^+ cells was determined using the Annexin V Apoptosis Detection Kit (BD Pharmingen) according to the manufacturer's protocol, with the exception that Annexin V-PE was used at a concentration of 2.5 μL in 100 μL of wash buffer. Detection of DNA fragmentation by TUNEL was determined using the FlowTACS kit (Trevigen) according to the manufacturer's protocol.

Antibodies. The following antibodies were used with the indicated specificity and appropriate combinations of fluorochromes: CD8α (clone 53-6.7; eBioscience), Thy1.1 (clone OX-7; BD Pharmingen), CD27 (clone LG.7F9; eBioscience), CD62L (clone MEL-14; BD Pharmingen), IFN-γ (clone XMG1.2; eBioscience), BrdU (clone PRB-1; eBioscience), Vα2 TCR (clone B20.1; eBioscience), Vβ8.1/2 TCR (clone MR5-2; BD Pharmingen), CD107a (clone 1D4B; BD Pharmingen), KLRG1 (clone 2F1; eBioscience), and CD127 (clone 7R34; eBioscience). Appropriate isotype controls were also used.

1. Nolz JC, Harty JT (2011) Protective capacity of memory CD8+ T cells is dictated by antigen exposure history and nature of the infection. *Immunity* 34:781–793.
2. Badovinac VP, Porter BB, Harty JT (2002) Programmed contraction of CD8(+) T cells after infection. *Nat Immunol* 3:619–626.
3. Jabbari A, Harty JT (2006) Simultaneous assessment of antigen-stimulated cytokine production and memory subset composition of memory CD8 T cells. *J Immunol Methods* 313:161–168.

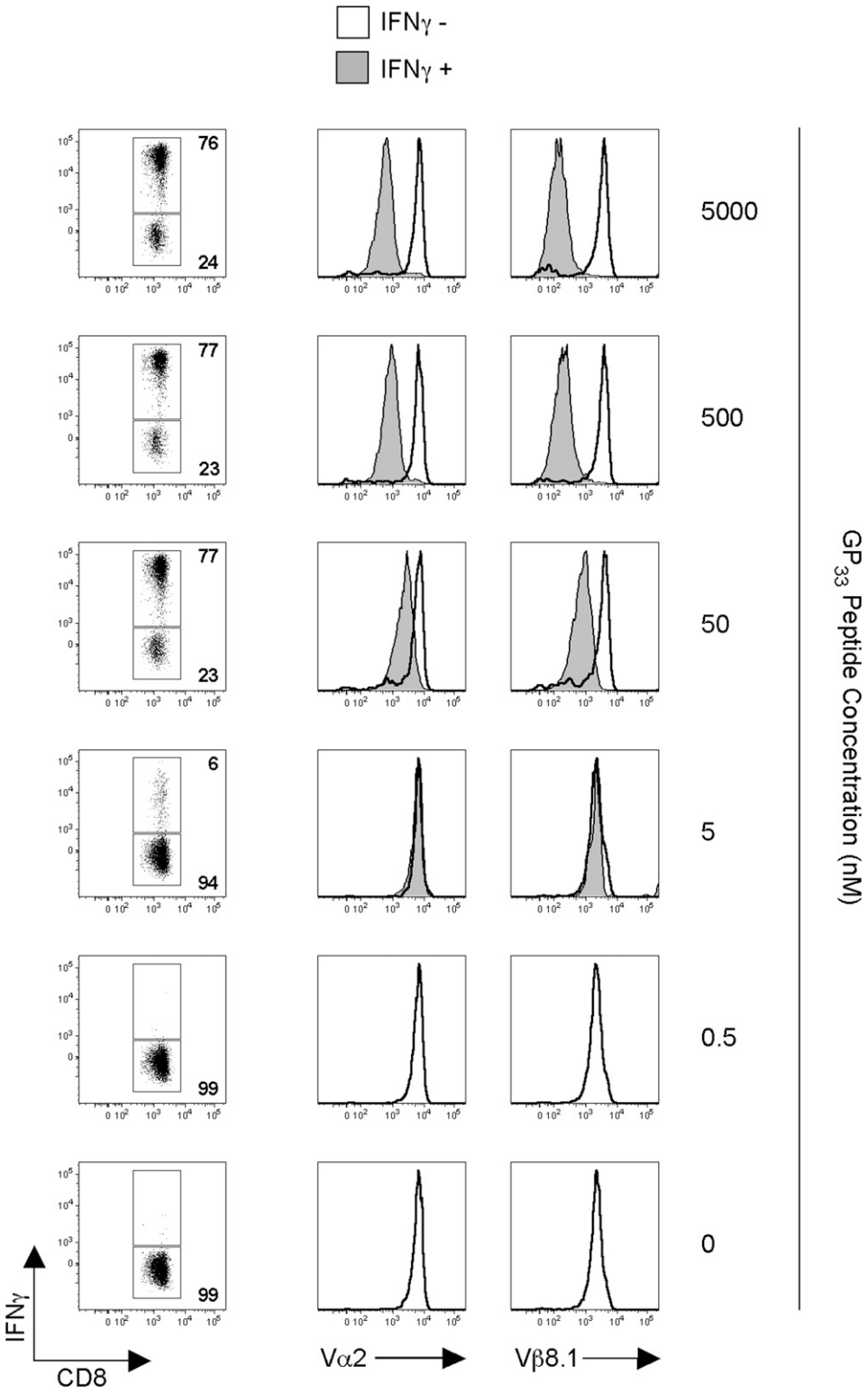

Fig. S1. IFN-γ production and TCR internalization on memory P14 CD8 T cells following stimulation with saturating amounts of $GP_{33–41}$ peptide. Total splenocytes containing memory P14 CD8 T cells (Thy1.1) were stimulated for 5 h with the indicated titrating amounts of $GP_{33–41}$ peptide. Memory P14 CD8 T cells were then analyzed for surface TCR expression (Vα2 and Vβ8.1) and IFN-γ production.

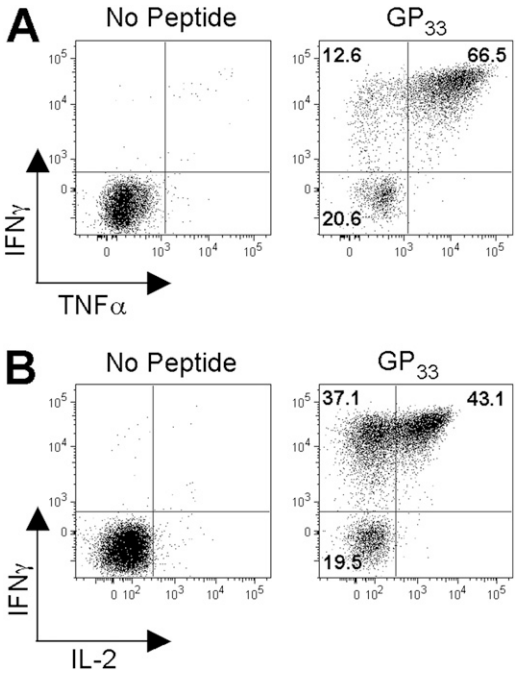

Fig. S2. Memory P14 CD8 T cells that do not produce IFN-γ also do not make TNF-α or IL-2. Total splenocytes containing memory P14 CD8 T cells (Thy1.1) were stimulated for 5 h with saturating amounts of $GP_{33–41}$ peptide. Memory P14 CD8 T cells were then analyzed for IFN-γ and TNF-α (*A*) or IL-2 (*B*) production.

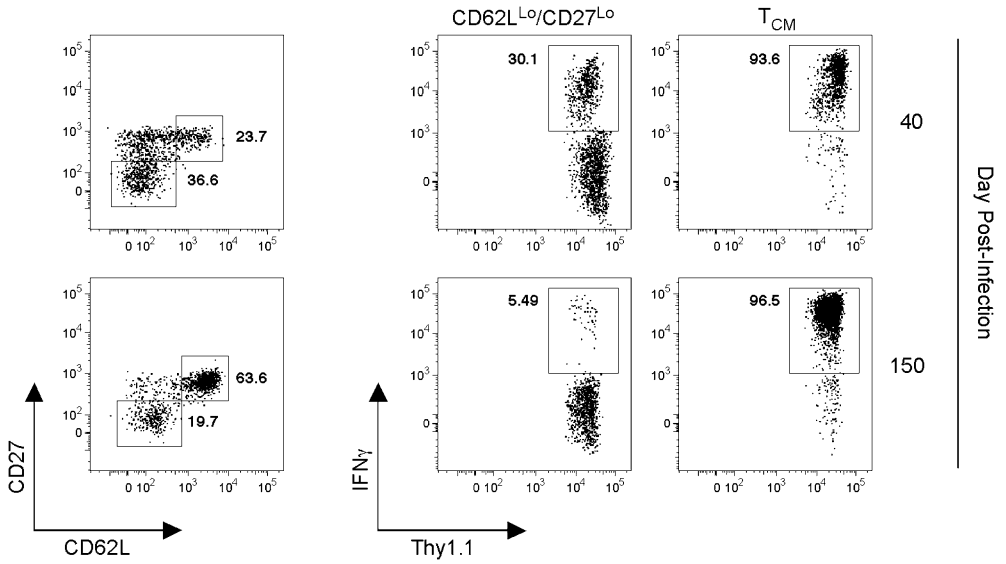

Fig. S3. Majority of $CD62L^{Lo}/CD27^{Lo}$ memory CD8 T cells found at late time points following infection do not make IFN-γ. 5×10^3 naive P14 CD8 T cells (Thy1.1) were transferred into naive B6 mice (Thy1.2) and subsequently infected with LCMV–Armstrong. On days 40 and 150 after infection, total splenocytes containing memory P14 CD8 T cells were stimulated with saturating amounts of $GP_{33–41}$ peptide for 5 h in the presence of *N*-(R)-(2-(Hydroxyaminocarbonyl) methyl)-4-methylpentanoyl-L-*t*-butyl-glycine-L-alanine 2-aminoethyl amide. Production of IFN-γ was then determined in the "central memory" ($CD62L^{Hi}/CD27^{Hi}$) and $CD62L^{Lo}/CD27^{Lo}$ populations.

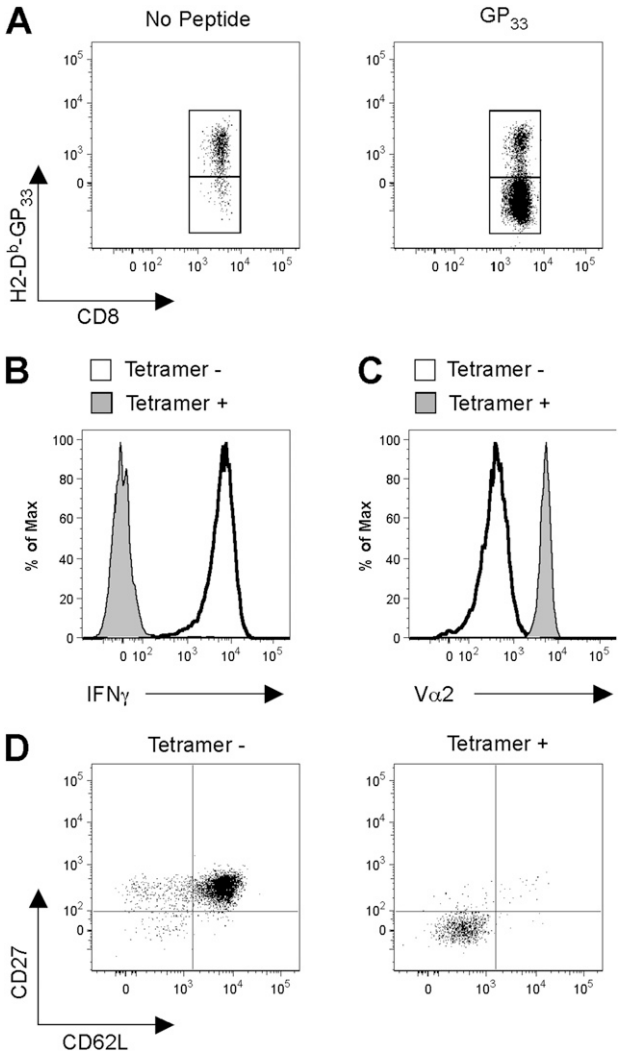

Fig. S4. Memory P14 CD8 T cells that do not make IFN-γ following stimulation with peptide can still be detected by tetramer staining. (*A*) Total splenocytes containing memory P14 CD8 T cells were stimulated for 5 h with saturating amounts of $GP_{33–41}$ peptide in the presence of N-(R)-(2-(Hydroxyaminocarbonyl) methyl)-4-methylpentanoyl-L-*t*-butyl-glycine-L-alanine 2-aminoethyl amide. Following stimulation, memory P14 CD8 T cells were analyzed for the ability to interact with H-$2D^b$-GP_{33} tetramer. Tetramer-positive and -negative cells following peptide stimulation in *A* were then analyzed for production of IFN-γ (*B*), Vα2, (*C*), and CD62L and CD27 (*D*).

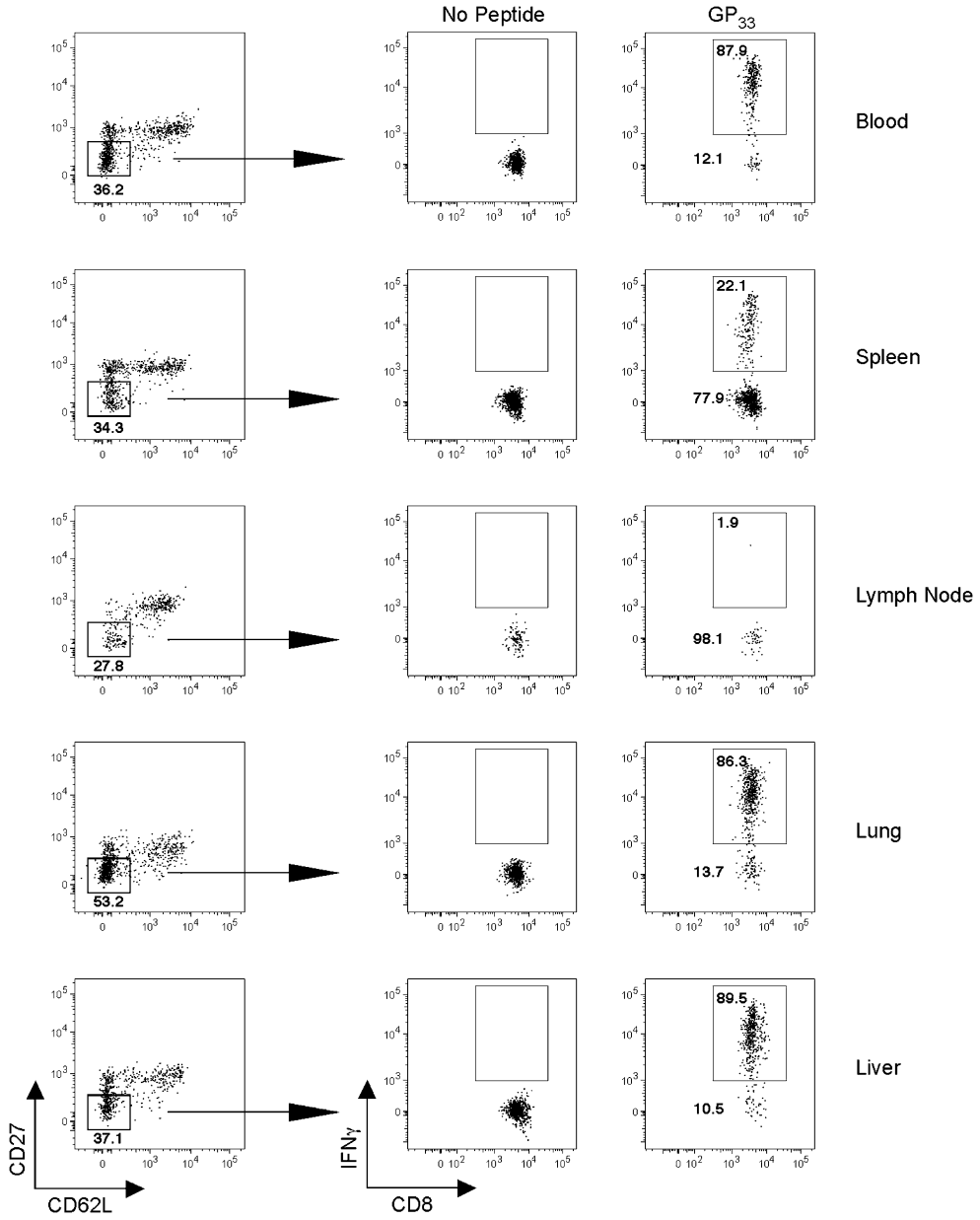

Fig. S5. Nonfunctional CD62L^{Lo}/CD27^{Lo} memory CD8 T cells are enriched in lymphoid organs. 5×10^3 naive P14 CD8 T cells were transferred into B6 mice and subsequently infected with LCMV–Armstrong. On day 50 after infection, CD62L^{Lo}/CD27^{Lo} memory P14 CD8 T cells from the indicated tissues were analyzed for the ability to produce IFN-γ following GP_{33-41} stimulation.